

Deactivation of Ruthenium Metathesis Catalysts via Facile Formation of Face-Bridged Dimers

Dino Amoroso, Glenn P. A. Yap, and Deryn E. Fogg*

Center for Catalysis Innovation and Research, Department of Chemistry, University of Ottawa, Ottawa, Ontario, Canada K1N 6N5

Received December 27, 2001

Reaction of $\text{RuCl}(\text{dcbp})(\mu\text{-Cl})_3\text{Ru}(\text{dcbp})(\text{N}_2)$ (**3**) with an excess of *tert*-butylacetylene at ambient temperatures yields the dinuclear monovinylidene $\text{RuCl}(\text{dcbp})(\mu\text{-Cl})_3\text{Ru}(\text{dcbp})(\text{L})$ (**4a**; $\text{L} = \text{C}=\text{CHBu}^t$, $\text{dcbp} = 1,4\text{-bis}(\text{dicyclohexylphosphino})\text{butane}$), rather than the expected mononuclear $\text{RuCl}_2(\text{dcbp})(\text{L})$. Attempted synthesis of an allenylidene derivative via the corresponding reaction with 1,1-diphenyl-2-propyn-1-ol stops at the stage of hydroxyvinylidene **4b** ($\text{L} = \text{C}=\text{CHC}(\text{OH})\text{Ph}_2$). While formation of these dinuclear products may be an artifact of low solubility, the corresponding monoalkylidene species **4c** ($\text{L} = \text{CHCH}=\text{CMe}_2$) is obtained on treating soluble $\text{RuH}(\text{dcbp})(\mu\text{-Cl})_2(\mu\text{-H})\text{Ru}(\text{dcbp})(\text{H}_2)$ (**5**) with 3-methyl-3-chloro-1-butyne. Formation of the perchloro species **4c** is consistent with facile homodimerization of the initially formed $\text{RuCl}_2(\text{dcbp})(\text{CHCH}=\text{CMe}_2)$ (**2d**), with expulsion of one alkylidene ligand as the free carbene. 2,7-Dimethylocta-2,4,6-triene, the formal product of carbene coupling, is observed by ^1H NMR. A minor product in this synthesis is proposed to be $\text{RuCl}(\text{dcbp})(\mu\text{-Cl})_2(\mu_2,\eta^1\text{-CHCH}=\text{CMe}_2)\text{RuCl}(\text{dcbp})$ (**8**). While the low activity of **4a**/**4b** in ring-opening metathesis polymerization of norbornene is attributable to their low solubility, that of **4c** points toward the stability of the $\text{Ru}_2(\mu\text{-Cl})_3$ entity. The low activity and facile formation of **4c** reveals an important deactivation pathway for catalysts of type **2d**, with additional relevance to other such chlororuthenium complexes, including systems of the Grubbs type. Product identities were established by ^1H , ^2H , ^{13}C , and ^{31}P NMR and IR spectroscopy and (for **4c** and **5**) by X-ray crystallography.

Introduction

Catalytic olefin metathesis by ruthenium complexes has received much attention, owing to the robustness and functional-group tolerance of the metal, and extraordinary success has accrued to benzylidene catalysts of the type $\text{RuCl}_2\text{LL}'(\text{CHPh})$ (**1a**, $\text{L} = \text{L}' = \text{PCy}_3$; **1b**, $\text{L} = \text{PCy}_3$, $\text{L}' = \text{imidazol-2-ylidene}$).¹ The high reactivity of the phenyldiazomethane reagent used to install the benzylidene ligand, and of the benzylidene functionality itself, has prompted considerable recent interest in alternative metal-carbon functionalities, including readily accessible ruthenium vinylidene and allenylidene derivatives.² The slower “turn-on” of such cumulenyliene species, vs benzylidene, may be advantageous where controlled reactivity is critical. The expected induction period in metathesis, arising from rates of initiation being slower than those of propagation, will increase polymer polydispersity in ring-opening

metathesis polymerization (ROMP),³ but will be manifested only as a latency period in ring-closing metathesis (RCM) or cross-metathesis. Indeed, a number of these species have shown promising activity in ROMP or RCM reactions.⁴

We⁵ and others^{6,7} have recently described the high ROMP activity of a new class of metathesis catalysts containing cis-chelating diphosphines. Among these, benzylidene complexes of the type $\text{RuCl}_2(\text{PP})(\text{CHR})$ ($\text{R} = \text{Ph}$; $\text{PP} = \text{dcbp}$ (1,4-bis(dicyclohexylphosphino)butane

(3) It may be noted that narrow polydispersities are not essential in many polymer applications, particularly structural ones; indeed, the precise specification of polymer properties that is associated with narrow molecular weight distributions can hamper polymer processing. See: Böhm, L. L.; Enderle, H. F.; Fleissner, M. *Stud. Surf. Sci. Catal.* **1994**, *89*, 351.

(4) Representative examples in ROMP: (a) Schwab, P.; Grubbs, R. H.; Ziller, J. W. *J. Am. Chem. Soc.* **1996**, *118*, 100. (b) Katayama, H.; Ozawa, F. *Chem. Lett.* **1998**, 67. (c) Katayama, H.; Yoshida, T.; Ozawa, F. *J. Organomet. Chem.* **1998**, *562*, 203. (d) Del Rio, I.; van Koten, G. *Tetrahedron Lett.* **1999**, *40*, 1401. (e) Saoud, M.; Romerosa, A.; Peruzzini, M. *Organometallics* **2000**, *19*, 4005. (f) Louie, J.; Grubbs, R. H. *Angew. Chem., Int. Ed.* **2001**, *40*, 1. In RCM: ref 4f. See also: (g) Schanz, H.-J.; Jafarpour, L.; Stevens, E. D.; Nolan, S. P. *Organometallics* **1999**, *18*, 5187. (h) Fürstner, A.; Liebl, M.; Lehmann, C. W.; Picquet, M.; Kunz, R.; Bruneau, C.; Touchard, D.; Dixneuf, P. H. *Chem. Eur. J.* **2000**, *6*, 1847. (i) Cetinkaya, B.; Demir, S.; Ozdemir, I.; Toupet, L.; Semeril, D.; Bruneau, C.; Dixneuf, P. H. *New J. Chem.* **2001**, *25*, 519. Indenylidene complexes have also proved metathesis active in RCM: ref 4g. See also: (j) Fürstner, A.; Guth, O.; Duffels, A.; Seidel, G.; Liebl, L.; Gabor, B.; Mynott, R. *Chem. Eur. J.* **2001**, *7*, 4811 and references therein. (k) Jafarpour, L.; Schanz, H.-J.; Stevens, E. D.; Nolan, S. P. *Organometallics* **1999**, *18*, 5416.

(5) (a) Amoroso, D.; Fogg, D. E. *Macromolecules* **2000**, *33*, 2815. (b) Amoroso, D.; Yap, G. P. A.; Fogg, D. E. *Can. J. Chem.* **2001**, *79*, 958.

* To whom correspondence should be addressed. E-mail: dfogg@science.uottawa.ca. Fax: (613) 562-5170.

(1) Recent reviews: (a) Trnka, T. M.; Grubbs, R. H. *Acc. Chem. Res.* **2001**, *34*, 18. (b) Jørgensen, M.; Hadwiger, P.; Madsen, R.; Stütz, A. E.; Wrodnigg, T. M. *Curr. Org. Chem.* **2000**, *4*, 565. (c) Roy, R.; Das, S. K. *J. Chem. Soc., Chem. Commun.* **2000**, 519. (d) Buchmeiser, M. R. *Chem. Rev.* **2000**, *100*, 1565. (e) Fürstner, A. *Angew. Chem., Int. Ed.* **2000**, *39*, 3012.

(2) For leading references to Ru allenylidene species, see: (a) Bruce, M. I. *Chem. Rev.* **1998**, *98*, 2797. (b) Cadierno, V.; Gamasa, M. P.; Gimeno, J. *Eur. J. Inorg. Chem.* **2001**, 571. Vinylidenes: (c) Bruneau, C.; Dixneuf, P. H. *Acc. Chem. Res.* **1999**, *32*, 311. (d) Bruce, M. I. *Chem. Rev.* **1991**, *91*, 197.

(**2a**), dpbb 1,4-bis(diphenylphosphino)butane; binap, (2,2'-bis(diphenylphosphino)-1,1'-binaphthyl)) represent the first Ru–diphosphine catalysts to exhibit high metathesis activity without ligand loss.⁵ A minimum turnover number (TON) of 2400 h⁻¹ was found for ROMP of norbornene via **2a**,^{5b} in which the diphosphine is the electron-rich, bulky, but flexible ligand dcybp. In contrast, comparably basic but rigid four- or five-membered chelate complexes (R = CHCH=CMe₂, PP = bis(di-*tert*-butylphosphino)methane (**2b**),^{6a,b} R = Ph, PP = 1,2-bis(di-*tert*-butylphosphino)ethane (**2c**),^{6c} R = Ph, PP = 1,2-bis(dicyclohexylphosphino)ethane^{6d}) displayed limited or zero activity prior to abstraction of chloride. We attribute the difference in catalytic behavior to the energetic accessibility in **2a** of a square-pyramidal geometry in which alkylidene lies in the basal plane and is thus *cis* to the entering monomer. Such a structure is supported by modeling and reactivity data. In contrast, spectroscopic, crystallographic, and modeling studies of the four- and five-membered chelate complexes indicate a strong structural preference for apical alkylidene, blocking the *cis* sites.⁶ While the activity of **2a** could potentially arise from dechelation of one end of the diphosphine ligand, the cumulative evidence suggests otherwise. Thus, no dangling phosphine is spectroscopically observable, no induction period is required in catalysis, and the polydispersity of the polymers produced (PDI ≈ 1.05) is lower than that found with **1a**.⁵ The last point implies that catalysis proceeds via a single species, with initiation rates exceeding rates of propagation. Preliminary indications of enhanced steric definition of the active site come from an increase in *cis* content of the polymer on use of the binap catalyst. Offsetting the high activity of these benzylidene species, however, was an instability that necessitated their generation *in situ*. Multiple decomposition products were observed in stoichiometric experiments, accompanied by extrusion of alkylidene as stilbene, consistent with the high reactivity of this functionality. We were thus interested in the possibility of installing alternative, more stable alkylidene or cumulenylidene ligands.

Results and Discussion

Ruthenium complexes containing bulky, electron-rich phosphines exhibit exceptionally high reactivity in metathesis^{1a,5b,6b} and hydrogenation^{8,9} catalysis. This

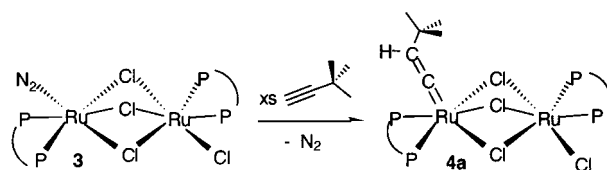
(6) Several groups have now described Ru–alkylidene complexes of type **2**, containing four- or five-membered chelating diphosphines, which are activated upon abstraction of halide. See: (a) Hansen, S. M.; Rominger, F.; Metz, M.; Hofmann, P. *Chem. Eur. J.* **1999**, *5*, 557. (b) Hansen, S. M.; Volland, M. A. O.; Rominger, F.; Eisenträger, F.; Hofmann, P. *Angew. Chem., Int. Ed.* **1999**, *38*, 1273. (c) Volland, M. A. O.; Straub, B. F.; Gruber, I.; Rominger, F.; Hofmann, P. *J. Organomet. Chem.* **2001**, *617*, 288. (d) Werner, H.; Jung, S.; Gonzalez-Herrero, P.; Ilg, K.; Wolf, J. *Eur. J. Inorg. Chem.* **2001**, 1957. More surprisingly, trigonal-bipyramidal analogues containing a 1,1'-bis(diphenylphosphino)ferrocene ligand^{6d} were also inactive prior to treatment with trimethylsilyl triflate. This is likely due, however, to the lower reactivity of arylphosphine derivatives, in conjunction with use of the low-ring-strain substrate cyclooctene.

(7) Six, C.; Beck, K.; Wegner, A.; Leitner, W. *Organometallics* **2000**, *19*, 4639.

(8) (a) Burk, M. J.; Martinez, J. P.; Feaster, J. E.; Cosford, N. *Tetrahedron* **1994**, *50*, 4399. (b) Burk, M. J. *Acc. Chem. Res.* **2000**, *33*, 363.

(9) (a) Drouin, S. D.; Zamanian, F.; Fogg, D. E. *Organometallics* **2001**, *20*, 5495. (b) Drouin, S. D.; Amoroso, D.; Yap, G. P. A.; Fogg, D. E. *Organometallics* **2002**, *21*, 1042.

Scheme 1



heightened reactivity can also be manifested as a susceptibility to alkylphosphine dehydrogenation, particularly in coordinatively unsaturated Ru precursors containing labile donors.^{5b,10} Thus, while dimeric [RuCl(dppb)]₂(μ-Cl)₂ is a tractable, readily isolable starting material,¹¹ its dcybp analogue undergoes exhaustive dehydrogenation of the alkylphosphine ligand under vacuum or argon.^{5b} “Placeholder” ligands are essential to restrain decomposition of the “RuCl₂(dcybp)” entity until a targeted ligand set (CHR, C=C_n=CHR, etc.) can be installed. Mixed-phosphine complexes such as RuCl₂(dcybp)(PPh₃) are limited in their utility, however, by the requirement for removal of liberated PPh₃.^{5a} Atom efficiency in such transformations is especially important in view of the tendency of alkylphosphine complexes to extremes of solubility, which can impede purification by recrystallization or trituration.^{4b,c,5} Dinitrogen is unique as a placeholder ligand in providing a labile, innocuous donor that does not offer alternative, undesired reaction pathways and does not contaminate the product. Dinuclear RuCl(dcybp)(μ-Cl)₃Ru(dcybp)(N₂) (**3**) thus provides an ideal entry point into dcybp chemistry.

Vinylidene Derivative. Vinylidene complexes, the simplest class of metallocumulenylenes M=(C=)_nCR₂ (*n* = 1), are readily accessible via reactions of transition-metal precursors with 1-alkynes.² Reaction of **3** with excess 3,3-dimethyl-1-butyne cleanly forms the dinuclear monovinylidene RuCl(dcybp)(μ-Cl)₃Ru(dcybp)(C=CH^tBu) (**4a**), with evolution of N₂ gas (Scheme 1). The identity of **4a** is established by detailed spectroscopic analysis and microanalytical data; no evidence of a mononuclear vinylidene species analogous to **2** is observed. Installation of vinylidene proceeds smoothly at room temperature (22 °C), despite the insolubility of both starting material and product. Thus, while addition of the alkyne reagent (0.5–4 equiv) to a stirred orange suspension of **3** in benzene did not effect dissolution, an aliquot removed after 12 h showed no remaining ³¹P NMR signals for **3**. Concentration of the solution and addition of pentane permitted isolation of orange **4a** in 86% yield. The proposed structure is supported by observation of a sharp, medium-intensity infrared band at 1633 cm⁻¹, a location characteristic^{2d} of the vinylidene ν_{C=C} vibration. ¹H NMR analysis reveals a triplet for the vinylidene proton (δ_H 3.06, ⁴J_{HP} = 3.8 Hz), accompanied by a peak for the *tert*-butyl protons at δ_H 1.24, visible as a sharp singlet above the broad, unresolved dcybp resonances (1.0–3.2 ppm). A diagnostic downfield triplet for the vinylidene α-carbon appears in the ¹³C{¹H} NMR spectrum (δ_C 352.1, ²J_{CP} = 16 Hz),

(10) (a) Borowski, A.; Sabo-Etienne, S.; Christ, M. L.; Donnadiou, B.; Chaudret, B. *Organometallics* **1996**, *15*, 1427. (b) Six, C.; Gabor, B.; Gorls, H.; Mynott, R.; Philipps, P.; Leitner, W. *Organometallics* **1999**, *18*, 3316.

(11) Joshi, A. M.; Thorburn, I. S.; Rettig, S. J.; James, B. R. *Inorg. Chim. Acta* **1992**, *198–200*, 283.

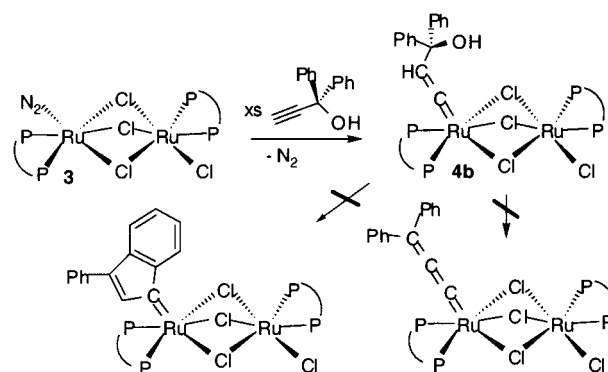
accompanied by a singlet for C_β at δ_C 119.7. $^{31}\text{P}\{^1\text{H}\}$ NMR data provide unequivocal evidence for the dinuclear monovinylidene structure. Four distinct sets of resonances of equal integrated intensity are observed, signifying the presence of four inequivalent phosphorus nuclei within a dinuclear structure devoid of symmetry (δ_P 50.6, 49.6 (ABq, $^2J_{PP} = 37$ Hz); 45.9, 40.1 (AB, $^2J_{PP} = 23$ Hz)).

Microanalytical data are in good agreement with the proposed structure, although low solubility precluded reprecipitation of **4a** from THF or aromatic (benzene, toluene) solvents. Purification by reprecipitation from methylene chloride or chloroform, in which the solubility is higher, is thwarted by the susceptibility of dcybp complexes to chlorination in such solvents. Mixed-valence, paramagnetic $\text{Ru}_2\text{Cl}_5(\text{dcypb})_2$ has been crystallographically identified among the products formed on dissolving **3** in CDCl_3 .^{5b} A new $^{31}\text{P}\{^1\text{H}\}$ NMR singlet (δ 46.8; ~ 2 –5%) is evident immediately after dissolving **4a** in CDCl_3 , though the timescale of decomposition is sufficiently slow that ^1H NMR data can be obtained without much difficulty on saturated solutions, and weak $^{31}\text{P}\{^1\text{H}\}$ NMR signals for **4a** can be discerned even after 7 days in solution.

3-Hydroxyvinylidene Derivative. Spontaneous dehydration of propyn-1-ols by transition-metal complexes provides an important route to allenylidene derivatives,^{2a,b,12} and in some cases their indenylidene isomers.^{4k,13} The reaction commonly proceeds via a 3-hydroxyvinylidene species, which on loss of water yields the allenylidene complex.^{2a,b} Addition of 1,1-diphenyl-2-propyn-1-ol (2 equiv) to a stirred suspension of **3** at room temperature caused a color change from orange to brown without dissolution; the ^{31}P NMR signals for starting **3** disappeared completely within 12 h. The light brown product was isolated in 88% yield by diluting the suspension with hexanes, filtering, and washing the powder with hexanes. As with **4a**, the insolubility of the complex precluded reprecipitation, and purification was effected by trituration with hexanes.

$^{31}\text{P}\{^1\text{H}\}$ NMR analysis of the product reveals four sets of resonances of equal intensity, in a pattern closely analogous to that for **4a** (51.5, 50.1 (ABq, $^2J_{PP} = 38$ Hz); 44.7 (d, unresolved), 40.9 (d, unresolved)), indicating formation of a complex of the type $\text{RuCl}(\text{dcypb})(\mu\text{-Cl})_3\text{Ru}(\text{dcypb})(\text{L})$. The infrared spectrum, however, does not show the diagnostic, strong allenylidene $\nu_{\text{C}=\text{C}}$ band between 1870 and 1970 cm^{-1} .^{2a,b} Indeed, this region of the spectrum is featureless: instead, a sharp, medium-intensity band is found at much lower energy (1644 cm^{-1}), suggesting the presence of a vinylidene (or indenylidene) ligand. The aromatic region of the ^1H NMR spectrum contains only a first-order splitting pattern for two equivalent, monosubstituted benzene rings, ruling out the possibility of isomerization of the allenylidene ligand to form a 3-phenyl-1-indenylidene^{4k} derivative (Scheme 2). The remainder of the spectrum reveals, in addition to the expected envelope for the dcybp protons from 0.8 to 3.5 ppm, two broad singlets

Scheme 2



at 4.38 and 3.99 ppm, each giving an integration of 1H. ^1H – ^{13}C HMQC experiments correlate the signal at δ_H 4.38 with an sp^2 carbon at 120 ppm. The signal at δ_H 3.99 does not correlate with any carbon nucleus; its identity as a hydroxyl proton is confirmed by exchange with D_2O and by observation of a medium-intensity $\nu(\text{OH})$ band at 3483 cm^{-1} in the IR spectrum of the protio derivative. From these data, we infer that installation of the allenylidene ligand has halted at the stage of hydroxyvinylidene **4b**.^{2a,b,14,15} A particular resistance of electron-rich Ru–hydroxyvinylidene species to dehydration has been suggested.^{2a,14} The ^1H NMR data, as well as the ^{13}C NMR shift position for C_β deduced from ^1H -detected HMQC experiments, are in excellent agreement with values reported for the related species $[\text{Cp}^*\text{Ru}\{\text{C}=\text{CHC}(\text{OH})\text{Ph}_2\}(\text{P}^i\text{Pr}_2\text{CH}_2\text{CH}_2\text{P}^i\text{Pr}_2)]\text{-}[\text{BPh}_4]$.¹⁴ Attempts to confirm the assignment by direct measurement of the $^{13}\text{C}\{^1\text{H}\}$ NMR spectrum were thwarted by the poor solubility of **4b** in benzene. The spectrum in CDCl_3 , though complicated by competing decomposition over the 24 h timescale required for good signal-to-noise ratios (vide supra), reveals the diagnostic downfield signals for the allenylidene moiety (C_α , δ 308.7, unresolved t; C_β , δ 243.4, s; C_γ , δ 150.4, s). Dissolution-triggered tautomerization of related hydroxyvinylidene species was recently described.¹⁴ This indirect evidence, with the cumulative weight of the ^1H NMR, HMQC, and infrared data, provides strong support for hydroxyvinylidene structure **4b**. Microanalytical data are in good agreement with this formulation.

Origin of Dinuclear Products. In principle, the dinuclear products of type **4** may be generated by an initially formed mononuclear species of the type $\text{RuCl}_2(\text{PP})(\text{C}=\text{C}=\text{CHR})$ via homodimerization (Scheme 3, path i), or via cross-dimerization¹⁶ with unreacted **3** (path ii). In view of the poor solubility of both **3** and **4a/4b**, however, we cannot rule out the alternative possibility that reaction takes place within the dinuclear framework, at a site vacated by N_2 (path iii).

In this context, installation of an alkylidene ligand via treatment of “ $\text{RuHCl}(\text{dcypb})$ ”¹⁷ with the propargyl chloride derivative 3-chloro-3-methyl-1-butyne¹⁸ (Scheme

(14) Bustelo, E.; Jiménez-Tenorio, M.; Puerta, M. C.; Valerga, P. *Eur. J. Inorg. Chem.* **2001**, 2391.

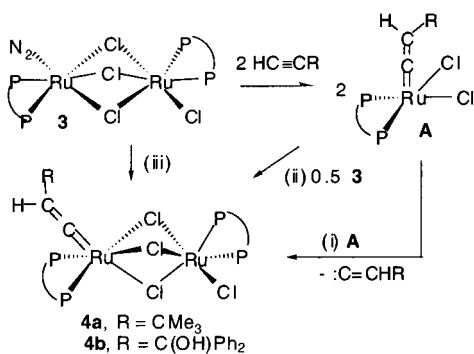
(15) (a) Touchard, D.; Dixneuf, P. H. *Coord. Chem. Rev.* **1998**, 178–180, 409. (b) Cadierno, V.; Gamasa, M. P.; Gimeno, J.; Gonzalez-Cueva, M.; Lastra, E.; Borge, J.; Garcia-Granda, S.; Perez-Carreño, E. *Organometallics* **1996**, 15, 2137. (c) Le Lagadec, R.; Roman, E.; Toupet, L.; Müller, U.; Dixneuf, P. H. *Organometallics* **1994**, 13, 5030.

(16) Ohm, M.; Schulz, A.; Severin, K. *Eur. J. Inorg. Chem.* **2000**, 2623.

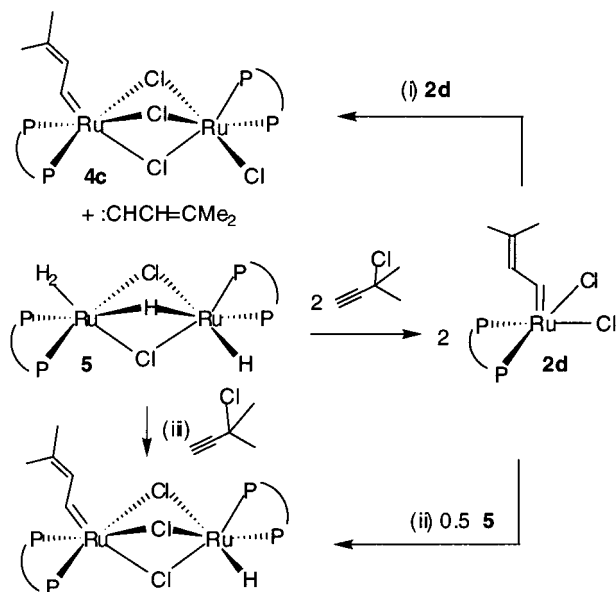
(12) Selegue, J. *Organometallics* **1982**, 1, 217.

(13) (a) Touchard, D.; Pirio, N.; Toupet, L.; Fettouhi, M.; Ouahab, L.; Dixneuf, P. H. *Organometallics* **1995**, 14, 5263. (b) Pirio, N.; Touchard, D.; Toupet, L.; Dixneuf, P. H. *J. Chem. Soc., Chem. Commun.* **1991**, 980. (c) Bruce, M. I.; Skelton, B. W.; White, A. H.; Zaitseva, N. N. *Inorg. Chem. Commun.* **1999**, 2, 17.

Scheme 3



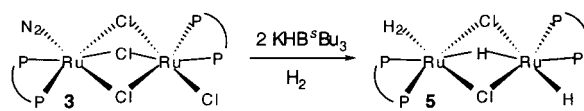
Scheme 4



4c is attractive for its mechanistic unambiguity. The extent of replacement of hydride by chloride offers direct insight into the probability of homodimerization (path i), vs paths ii and iii. Furthermore, installation of one alkylidene concomitant with each chloride ligand means that formation of monoalkylidene **4c** ($\text{RuCl}(\text{dcbp})(\mu\text{-Cl})_3\text{Ru}(\text{dcbp})(\text{CHCH}=\text{CMe}_2)$) would necessarily implicate homodimerization. Conversely, if formation of **4a/4b** occurs via path iii and dimerization of the mononuclear complexes $\text{RuCl}_2(\text{PP})(\text{L})$ is disfavored (as indeed suggested by the stability^{6b} of **2b,c**), we considered that the propargyl chloride route might afford access to $\text{RuCl}_2(\text{dcbp})(\text{CHCH}=\text{CMe}_2)$ (**2d**).

Dcbp Hydrides. Exploration of the propargyl chloride route requires prior synthesis of the hydrido chloro dimer **5**, $\text{Ru}(\text{H})(\text{dcbp})(\mu\text{-Cl})_2(\mu\text{-H})\text{Ru}(\text{dcbp})(\eta^2\text{-H}_2)$.¹⁷ The latter is cleanly obtained by reaction of **3** with KHB^tBu_3 (Scheme 5); disproportionation to a polyhydride does not occur, in contrast to the behavior of dichlorocarbonyl species $[\text{RuCl}_2(\text{dcbp})(\text{CO})]_2$.^{9b} Suspensions of **3** react rapidly with 2 equiv of KHB^tBu_3 in benzene under 1 atm of H_2 (room temperature, <5 min), yielding a homogeneous orange solution. Detailed NMR

Scheme 5

Table 1. Properties of Hydride Signals for **5** at 194 K and 500 MHz

	δ_{H}		
	-9.8	-12.6	-20.3
integration	1H	2H	1H
T_1 , ms	200	60	450
assign	$\text{Ru}(\mu_2, \eta^1\text{-H})$	$\text{Ru}(\eta^2\text{-H}_2)$	$\text{Ru}(\eta^1\text{-H})$

studies, supported by X-ray crystallography, confirm the formation of **5**. This species is also formed on hydrolysis and hydrogenolysis of the Ru-silylene derivative $\text{RuCl}(\eta^3\text{-dcbp})(\text{SiL}^{\text{N}_2})$ ($\text{SiL}^{\text{N}_2} = 1,3\text{-di-tert-butyl-1,3,2-diazasilol-2-ylidene}$).¹⁹

³¹P NMR analysis of **5** (C_6D_6 , 22 °C) reveals two broad singlets, at 65 and 52 ppm (1:1 ratio; $\omega_{1/2} = 57.8$ and 173.7 Hz, respectively). These signals do not couple to each other (³¹P-³¹P COSY) but are correlated by ³¹P EXSY NMR. The upfield resonance broadens into the baseline on cooling to 276 K, while the signal at $\delta_{\text{P}} 65$ sharpens. Little further change occurs down to 180 K, at which temperature two broad signals ($\delta_{\text{P}} 78$, 21) emerge, each giving an integration of approximately half the intensity of the resonance still apparent at 63 ppm. This behavior is characteristic of $\text{Ru}(\text{H})(\text{PP})(\mu\text{-Cl})_2(\mu\text{-H})\text{Ru}(\text{PP})(\eta^2\text{-H}_2)$ species: directly analogous spectra have been described for triphenylphosphine and tri-*p*-tolylphosphine complexes.²⁰ The broad upfield peak in these species is assigned to the “Ru-H₂” end of the molecule, at which the terminal dihydrogen ligand undergoes rapid exchange with bridging hydride. While the breadth of this signal precludes observation of a hydride correlation in ¹H-³¹P HMQC experiments,²¹ ¹H NMR analysis of **5** (C_7D_8 , 22 °C) is in excellent agreement with the literature reports.²⁰ A single hydride resonance appears ($\delta_{\text{H}} -13.8$, br s), which on cooling to 194 K coalesces into three broad resonances (Table 1). No improvement in resolution occurs down to 170 K. Integration and T_1 values are consistent with the presence of two hydride ligands and a single $\text{Ru}(\eta^2\text{-H}_2)$ moiety.

Crystal Structure of 5. Several small crystals of **5** formed at the gas-solution interface of a benzene solution of **5** on storage under H_2 , one of which was found suitable for X-ray analysis. An ORTEP representation appears in Figure 1, with crystallographic and selected structural parameters in Tables 2 and 3, respectively. All hydride ligands were located and refined with a riding model. Complex **5** adopts a diruthenium structure, in which the two metal centers

(19) Amoroso, D.; Haaf, M.; Yap, G. P. A.; West, R.; Fogg, D. E. *Organometallics* **2002**, *21*, 534.

(20) (a) Hampton, C.; Cullen, W. R.; James, B. R.; Charland, J.-P. *J. Am. Chem. Soc.* **1988**, *110*, 6918. (b) Hampton, C. R. S. M.; Butler, I. R.; Cullen, W. R.; James, B. R.; Charland, J.-P.; Simpson, J. *Inorg. Chem.* **1992**, *31*, 5509. (c) Hampton, C.; Dekleva, T. W.; James, B. R.; Cullen, W. R. *Inorg. Chim. Acta* **1988**, *145*, 165.

(21) For successful correlation by HMQC experiments, the peak width in Hz must be less than the value of the heteronuclear coupling constant. While exchange masks the ¹H-³¹P coupling within **5**, the expected ²J_{HP} value of 2–4 Hz is very small relative to the peak width of 40 Hz.

(17) Neither the 14-electron, mononuclear species $\text{RuHCl}(\text{dcbp})$ nor the corresponding 16-electron dimer is attainable, but the H_2 -stabilized dimer $\text{Ru}(\text{H})(\text{dcbp})(\mu\text{-Cl})_2(\mu\text{-H})\text{Ru}(\text{dcbp})(\eta^2\text{-H}_2)$ (**5**; cf. **3**) provided a suitable alternative (vide infra).

(18) Wilhelm, T. E.; Belderrain, T. R.; Brown, S. N.; Grubbs, R. H. *Organometallics* **1997**, *16*, 3867.

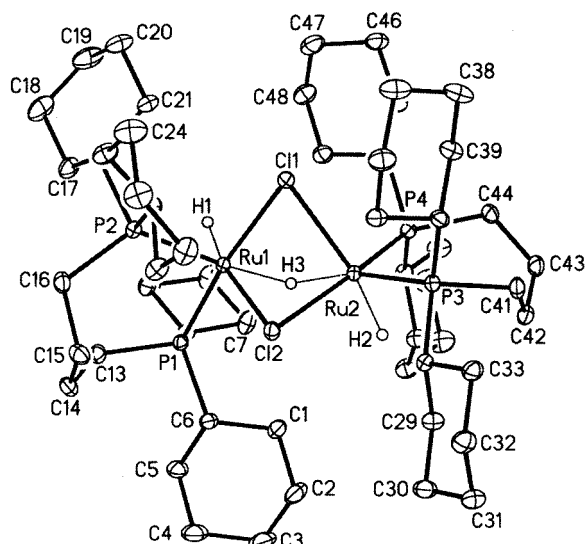


Figure 1. ORTEP diagram of Ru(H)(dcypb)(μ -Cl) $_2$ (μ -H)-Ru(dcy pb)(η^2 -H $_2$) (**5**) with thermal ellipsoids shown at the 30% probability level. Non-hydridic hydrogen atoms and solvate molecules are omitted for clarity.

Table 2. Crystal Data and Structure Refinement Details for 5

empirical formula	C $_{68}$ H $_{120}$ Cl $_2$ P $_4$ Ru $_2$
fw	1334.56
temp	203(2) K
wavelength	0.710 73 Å
cryst syst, space group	triclinic, $P\bar{1}$
unit cell dimens	$a = 11.2119(7)$ Å $b = 13.6190(9)$ Å $c = 24.6084(16)$ Å $\alpha = 77.5280(10)^\circ$ $\beta = 79.2950(10)^\circ$ $\gamma = 68.6670(10)^\circ$
V	3393.7(4) Å 3
Z , calcd density	2, 1.306 mg/m 3
abs coeff	0.656 mm $^{-1}$
$F(000)$	1420
cryst size	0.30 \times 0.12 \times 0.07 mm
θ range for data collec	1.63–28.73°
limiting indices	$-14 \leq h \leq 14$, $-17 \leq k \leq 18$, $0 \leq l \leq 33$
no. of rflns collected/unique	26 599/15 369 ($R(\text{int}) = 0.0187$)
completeness to $\theta = 28.73^\circ$	87.3%
abs cor	semiempirical from equivalents
max and min transmissn	0.928074 and 0.861365
refinement method	full-matrix least squares on F^2
no. of data/restraints/params	15 369/0/694
goodness of fit on F^2	1.012
R^a	0.0273
R_w^b	0.0385

$$^a R = \sum ||F_o| - |F_c|| / \sum |F_o|, \quad ^b R_w = [\sum w\delta^2 / \sum wF_o^2]^{1/2}.$$

have a distorted-octahedral geometry, bridged by two chloride ligands and one hydride ligand. The diffraction data indicate 50% site occupancy of two terminal sites by hydride and η^2 -H $_2$. The “Ru-H” (terminal) distances (ca. 1.57(2) Å) are thus intermediate between values expected for Ru–H and Ru–H $_2$: cf. values of 1.75(3) Å for the Ru–(η^2 -H $_2$) distance in the chloride-bridged dimer Ru(η^2 -H $_2$)(dppb)(μ -Cl) $_3$ RuCl(dppb) 22 and 1.50(4) Å for the terminal Ru–H distance in Ru(H)-(PPh $_3$) $_2$ (μ -Cl) $_2$ (μ -H)Ru(L $_2$)(η^2 -H $_2$) (**6**; L $_2$ = Fe(η^5 -C $_5$ H $_3$ -CHMeNMe $_2$)P i Pr) $_{2,1,2}$ (η^5 -C $_5$ H $_5$) 20), in which no such

Table 3. Selected Bond Lengths (Å) and Angles (deg) for 5

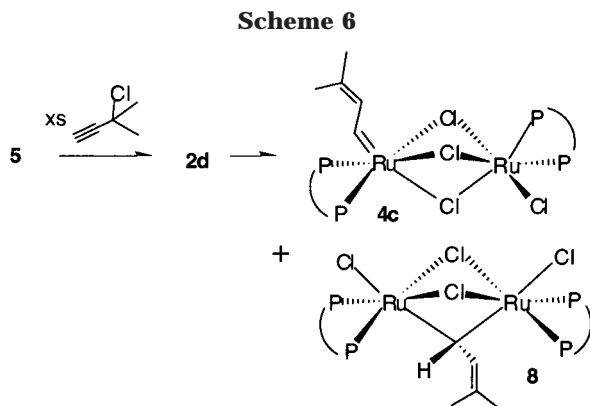
Ru(1)–P(1)	2.2681(5)	Ru(2)–P(3)	2.2543(5)
Ru(1)–P(2)	2.3854(5)	Ru(2)–P(4)	2.2453(5)
Ru(1)–H(1)	1.573(13)	Ru(2)–H(2)	1.559(12)
Ru(1)–H(3)	1.768(18)	Ru(2)–H(3)	1.84(2)
Ru(1)–Cl(1)	2.4725(5)	Ru(2)–Cl(1)	2.5531(5)
Ru(1)–Cl(2)	2.4298(5)	Ru(2)–Cl(2)	2.5034(5)
Ru(1)–Ru(2)	2.8595(3)		
P(1)–Ru(1)–P(2)	100.384(17)	P(4)–Ru(2)–P(3)	98.762(19)
Ru(1)–Cl(1)–Ru(2)	69.337(12)	Ru(1)–Cl(2)–Ru(2)	70.832(14)
P(1)–Ru(1)–Cl(1)	171.687(17)	P(4)–Ru(2)–Cl(2)	166.667(19)
P(2)–Ru(1)–H(3)	173.2	P(3)–Ru(2)–H(3)	167.1
H(1)–Ru(1)–Cl(2)	168.3	H(2)–Ru(2)–Cl(1)	169.5
Ru(1)–H(3)–Ru(2)	104.6(9)		

disorder exists. Likewise, the strong trans effect of hydride, relative to η^2 -H $_2$, will normally cause lengthening of the Ru–Cl bond trans to the hydride ligand. However, the presence in **5** of a statistical distribution of hydride and dihydrogen ligands trans to μ -Cl results in a narrower range in bond lengths relative to those in **6**: cf. values of 2.4298(5)–2.5531(5) Å in **5** vs 2.435(2)–2.620(2) Å in **6**.

Despite formation of a few small crystals of **5** as described above, repeated efforts to isolate this species proved unsuccessful. Its high solubility inhibited precipitation from all solvents investigated, including cold (–35 °C) pentane. As with other dcy pb complexes, concentration to dryness results in decomposition. We have described the susceptibility of the parent complex **3** to intramolecular dehydrogenation under vacuum or argon. 5b Intramolecular decomposition also occurs on stripping solutions of **5** to dryness, as indicated by the serendipitous crystallization of [Ru(H)(dcypb)(μ -Cl) $_3$ -Ru(dcy pb)(N $_2$)] (**7**), containing an additional chloride ligand, from the large number of species formed. We have reported the crystal structure of **7**. 19 Attempts to circumvent dehydrogenation by drying **5** under a stream of H $_2$ were unsuccessful, decomposition to many products again being indicated by NMR analysis. Microanalysis carried out on the solid products, on the possibility that decomposition ensues on redissolution, gave results consistently low in carbon. As with complex **3**, however, **5** can be synthesized and handled without difficulty in solutions saturated with an appropriate, stabilizing donor ligand. For all subsequent synthetic efforts, **5** was therefore prepared and reacted in situ under H $_2$.

Alkylidene Derivatives. Reaction of a homogeneous orange solution of **5** with 3-chloro-3-methyl-1-butyne resulted in immediate formation of the dinuclear monoalkylidene RuCl(dcy pb)(μ -Cl) $_3$ Ru(dcy pb)(CHCH=CMe $_2$) (**4c**; Schemes 4 and 6), the identity of which was confirmed by NMR and crystallographic analysis. In contrast to **4a/4b**, the complex exhibits good solubility, aiding its spectroscopic characterization. It is isolated in ca. 80% yield on reprecipitation from benzene–hexanes, though contaminated with ca. 20% of coproduct **8** (vide infra) which could not be separated by reprecipitation or washing. No other products are spectroscopically evident. Four $^{31}\text{P}\{^1\text{H}\}$ NMR resonances, of equal integrated intensity, are found for **4c**, signifying the presence of four inequivalent phosphorus nuclei within a dinuclear complex devoid of symmetry. At room temperature in C $_6$ D $_6$, these resonances are broad,

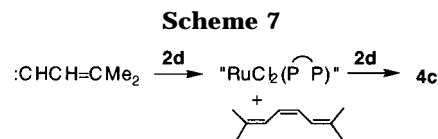
(22) Joshi, A. M.; James, B. R. *J. Chem. Soc., Chem. Commun.* **1989**, 1785.



unresolved singlets (δ 54.0, 46.1, 45.1, 42.9). On cooling to 273 K (C_{7D_8}), the signal at ca. 43 ppm sharpens to a doublet ($^2J_{PP} = 32$ Hz), but the others remain unresolved: on cooling further, all four signals broaden until (245 K) they are nearly lost in the baseline. In $CDCl_3$, these signals resolve into pairs of doublets (δ 59.0, 43.7 (AB, $^2J_{PP} = 39$ Hz); δ 46.9, 40.5 (AB, $^2J_{PP} = 26$ Hz)), in a pattern closely similar (including J values) to those found for **4a/4b**, particularly for the upfield pair of doublets. The latter resonances are therefore assigned to the “Cl-end” of the dimer. Reaction with solvent also occurs, however, affording an unidentified product characterized by a pair of doublets at δ_P 46.4, 42.6 ($^2J_{PP} = 35$ Hz). One of the accessible reaction paths involves chlorination, as indicated by crystallization of paramagnetic $Ru_2Cl_5(dcpypb)_2$ (identified by comparison of the unit cell to that previously^{5b} established) within 48 h of dissolution in $CDCl_3$.

1H NMR analysis of **4c** in C_6D_6 reveals a quartet for H_α of the alkylidene (δ_H 16.92, q, $^3J = 11.5$ Hz). The multiplicity of this signal indicates coupling to two phosphorus nuclei and H_β with coincident $^3J_{HH}$ and $^3J_{HP}$ values (as earlier found^{6b} for **2b**). Complex **4c** is observed irrespective of reaction time, stoichiometry (2–20 equiv), or temperature (-35 °C or room temperature), providing strong evidence for facile homodimerization of initially formed **2d** (Scheme 4, path i). The triene $Me_2C=CHCH=CHCH=CMe_2$ is observed by 1H NMR as the organic coproduct.²³ The latter “carbene coupling” product is unlikely to arise from direct reaction of two free, highly reactive carbenes, which are expected to be present in low concentration,^{23a} but may rather occur via attack of carbene on precursor **2d** (Scheme 7).

The byproduct **8** also contains an $Ru(dcpypb)(CHCH=CMe_2)$ entity, as indicated by observation of a $^{31}P\{^1H\}$ NMR singlet at δ_P 43.4, which is correlated in $^1H-^{31}P$ HMQC experiments with an alkylidene quartet (H_α ; δ_H 15.83, $^3J_{HH} = ^3J_{HP} = 12.0$ Hz). The equivalence of the



phosphorus nuclei indicates a higher degree of symmetry than in **4c**; this does not appear to be due to averaging of environments through a fluxional process, as low-temperature ^{31}P NMR studies show no change (other than minimal peak broadening) from 333 to 203 K. The NMR data are consistent with the square-pyramidal structure **2d**, containing apical alkylidene and equivalent, cis phosphine ligands. However, this mononuclear formulation is difficult to reconcile with the instability toward dimerization implied by formation of **4c**, especially given the persistence of the singlet at δ_P 43.4 in NMR spectra recorded over 7 days in solution. The latter evidence strongly suggests that the species responsible is not on the reaction path leading to **4c**, but that both it and **4c** arise from dimerization of mononuclear **2d**.

An alternative structural possibility is an isomer of **4c**, containing a bridging alkylidene ligand (**8**, Scheme 7), potentially formed by nucleophilic attack of the electron-rich metal at C_α . Precedent for such a rearrangement is found in crystallographically characterized $Cp^*Ru(\mu-Cl)_2(\mu,\eta^1-CHCH=CPh_2)RuCp^*$, in which the bridging alkylidene lies perpendicular to the Ru–Ru vector.²⁴ Observation of a quartet for H_α in **8** implies a similar geometry, in which the plane containing C_α and the two terminal chloride ligands bisects the P–Ru–P vector, and a near 90° dihedral angle exists between H_α and one ^{31}P nucleus of each dcpypb ligand.²⁵ Attempts to confirm this structure by $^{13}C\{^1H\}$ NMR analysis were hampered by the low solubility of **8**, but observation of a poorly resolved multiplet containing five principal lines at δ_C 308.6 for C_α (cf. a well-resolved triplet for the corresponding carbon nucleus in **4c**) is consistent with an A_2B_2X spin system, in which $J_{P(A)-C} \neq J_{P(B)-C}$.

Crystal Structure of 4c. Crystals of **4c** were obtained by slow evaporation of toluene solutions layered with hexanes. An ORTEP drawing is shown in Figure 2. Structural parameters are collected in Table 4 and key bond lengths and angles in Table 5. Complex **4c** adopts a triply chloride bridged diruthenium structure, in which the coordination geometry at each metal center is distorted octahedral. The structure is unsymmetrical, with Ru(1) bearing an alkylidene functionality and Ru(2) a chloride ligand. Complex **4c** represents the first crystallographically characterized example of a dinuclear Ru phosphine complex containing a single, terminal alkylidene moiety; importantly, it also demonstrates the accessibility of the face-bridged geometry in these systems. One prior report of a diruthenium monoalkylidene complex has appeared, for which a doubly chloride bridged structure, $RuCl(p\text{-cymene})(\mu-Cl)_2RuCl(PCy_3)(CHCH=CMe_2)$, was proposed.²⁶ The apparent failure of **2b, c** to form face-bridged biotetrahedra of type **4** may be due to geometric and steric constraints

(23) (a) Given the high reactivity of the carbene (Smith, M. B.; March, J. *March's Advanced Organic Chemistry*, 5th ed.; Wiley: New York, 1994; p 252), other organic byproducts may also be expected. However, the major peaks in the olefinic region are due to the complex AA'BB' patterns for 2,7-dimethylocta-2,4,6-triene (4E and 4Z isomers). Chemical shifts agree with values reported (see, for example: tom Dieck, H.; Keinzel, A. *Angew. Chem., Int. Ed. Engl.* **1979**, *18*, 324; Cao, X.-P.; Chan, T.-L.; Chow, H.-F.; Tu, J. *J. Chem. Soc., Chem. Commun.* **1995**, 1297), while the patterns correspond precisely to those calculated using the ACD/HNMR software program. For a representation of calculated and experimental data for this triene obtained in the course of related work, see ref 23b. (b) Following submission of this paper, identical dimerization chemistry was confirmed for the useful precursor complex $RuCl_2(PPh_3)_2(CHCH=CMe_2)$: Amoroso, D.; Snelgrove, J. L.; Conrad, J.; Yap, G. P. A.; Fogg, D. E. *Adv. Synth. Catal.*, in press.

(24) Gagné, M. R.; Grubbs, R. H.; Feldman, J.; Ziller, J. W. *Organometallics* **1992**, *11*, 3933.

(25) The alkylidene resonance for $RuCl_2(PCy_3)_2(CHPh)$ likewise appears as a singlet, rather than the triplet found for the PPh_3 analogue.^{4a}

(26) Dias, E. L.; Grubbs, R. H. *Organometallics* **1998**, *17*, 2758.

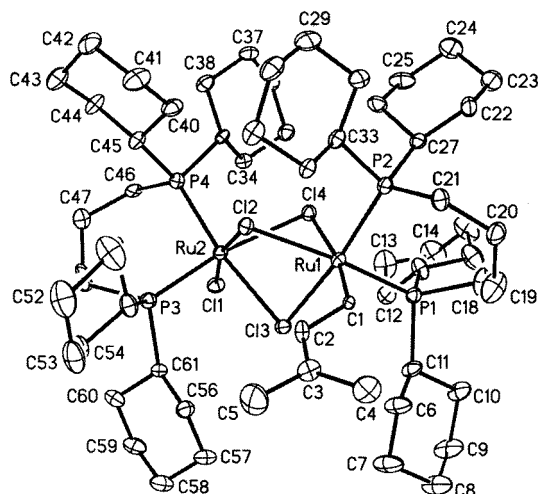


Figure 2. ORTEP diagram of $\text{RuCl}(\text{dcybp})(\mu\text{-Cl})_3\text{Ru}(\text{dcybp})[\text{CHCH}=\text{CMe}_2]$ (**4c**) with thermal ellipsoids shown at the 30% probability level. Hydrogen atoms and solvate molecule are omitted for clarity.

Table 4. Crystal Data and Structure Refinement Details for 4c

empirical formula	$\text{C}_{64}\text{H}_{119}\text{Cl}_4\text{P}_4\text{Ru}_2$
fw	1356.41
temp	203(2) K
wavelength	0.710 73 Å
cryst syst, space group	triclinic, $P\bar{1}$
unit cell dimens	$a = 11.7069(16)$ Å $b = 14.1411(19)$ Å $c = 22.140(3)$ Å $\alpha = 95.066(3)^\circ$ $\beta = 93.018(2)^\circ$ $\gamma = 112.186(2)^\circ$
V	$3365.9(8)$ Å ³
Z , calcd density	2, 1.338 mg/m ³
abs coeff	0.739 mm ⁻¹
$F(000)$	1438
cryst size	$0.12 \times 0.10 \times 0.01$ mm
θ range for data collec	$1.57\text{--}20.82^\circ$
limiting indices	$-11 \leq h \leq 11$, $-14 \leq k \leq -14$, $0 \leq l \leq 22$
no. of rflns collected/unique completeness to $\theta = 20.82^\circ$	26256/7055 ($R(\text{int}) = 0.1233$) 99.8%
abs cor	semiempirical from equivalents
max and min transmission	0.928 076 and 0.598 612
refinement method	full-matrix least squares on F^2
no. of data/restraints/params	7055/579/667
goodness of fit on F^2	1.038
R^a	0.0540
R_w^b	0.1076

$$^a R = \sum ||F_o| - |F_c|| / \sum |F_o|, \quad ^b R_w = [\sum w\delta^2 / \sum wF_o^2]^{1/2}.$$

Table 5. Selected Bond Lengths (Å) and Angles (deg) for 4c

Ru(1)–C(1)	1.888(8)	Ru(1)–Cl(3)	2.451(2)
Ru(1)–P(1)	2.304(3)	Ru(1)–Cl(4)	2.543(2)
Ru(1)–P(2)	2.320(2)	Ru(2)–Cl(1)	2.398(2)
Ru(2)–P(3)	2.257(3)	Ru(2)–Cl(2)	2.400(2)
Ru(2)–P(4)	2.277(2)	Ru(2)–Cl(3)	2.525(2)
Ru(1)–Cl(2)	2.471(2)	Ru(2)–Cl(4)	2.532(2)
C(1)–Ru(1)–Cl(4)	170.0(3)	P(4)–Ru(2)–Cl(3)	170.33(9)
P(2)–Ru(1)–Cl(3)	173.33(8)	P(3)–Ru(2)–P(4)	96.95(9)
P(1)–Ru(1)–Cl(2)	169.43(8)	Ru(2)–Cl(2)–Ru(1)	88.43(8)
P(1)–Ru(1)–P(2)	94.31(9)	Ru(1)–Cl(3)–Ru(2)	86.12(7)
Cl(1)–Ru(2)–Cl(2)	166.89(8)	Ru(2)–Cl(4)–Ru(1)	84.04(7)
P(3)–Ru(2)–Cl(4)	167.92(7)		

associated with their rigid, bulky chelate rings. On abstraction of halide from **2b**, the edge-bridged bipyramidal dimer is formed.^{6b}

Table 6. Ru-Catalyzed ROMP of Norbornene^a

entry	cat.	additive ^b	conversn (%)	time (min)
1	4c/8		81	60
2	4c/8	TMS-OTf	87	5
3	4c/8	PhCHN ₂	100	5
4	4a		27	1140
5	4a	TMS-OTf	90	1200
6	4b		99	478
7	4b	TMS-OTf	92	1353

^a Reaction conditions: CDCl_3 solvent, $[\text{norbornene}]:[\text{Ru}_2] = 225$; 1, $[\text{Ru}_2] = 3.2$ mM, room temperature (22°C). ^b Additives: 3.2 mM TMS-OTf or PhCHN₂.

The Ru–C distance in **4c** is similar to that described^{6b} for mononuclear alkylidene species **2b** (1.888 Å for **4c** vs 1.858 Å for **2b**). The most significant difference between the two structures appears in the P–Ru–P angles, which are ca. 20° greater in **4c**, reflecting the flexibility associated with the four-carbon, vs one-carbon, diphosphine backbone. Non-alkylidene bond lengths and angles within the $\text{RuCl}(\text{PP})(\mu\text{-Cl})_3\text{Ru}(\text{PP})(\text{L})$ skeleton compare well with those reported for $\text{RuCl}(\text{dppb})(\mu\text{-Cl})_3\text{Ru}(\text{dppb})(\text{L})$ ($\text{L} = \text{dmsO}$,¹¹ H_2). Ru–P bond lengths are very slightly longer for **4c** (average 2.29 Å vs 2.28 Å); Ru($\mu\text{-Cl}$)₃Ru angles are ca. 3° larger (average 86.20°), reflecting the higher steric demand of the dcybp entity.

Catalysis. In striking contrast to the parent system **2a**, dinuclear **4c/8** exhibits very low metathesis activity, even toward reactive substrates such as norbornene (NBE). Thus, while ROMP of 200 equiv of NBE in CDCl_3 using **2a** is complete before the time of first measurement (5 min, minimum TON 2400 h⁻¹; vide supra), an identical catalytic run carried out with **4c/8** is still incomplete after 1 h (Table 6, entry 1; TON 180 h⁻¹). We attribute this low reactivity to the thermodynamic stability of the *face-bridged* structure. We note that facile bridge cleavage, leading to very high metathesis activity, has been reported for the edge-bridged dtbpm dimer.^{6b} High activity can be restored in the present systems by abstraction of chloride from **4c/8** with trimethylsilyl triflate (TMS-OTf; 1 equiv per dimer) or by bridge cleavage via addition of 1.0 equiv of PhCHN₂ per dimer,²⁷ installing a second alkylidene functionality.

Complexes **4b** and **4a** display even lower metathesis activity, but their very low solubility precludes establishment of any correlation between alkylidene/cumulenyldene structure and activity. In all cases, the solutions became highly viscous as the reaction progressed, and the polymers were insoluble once isolated, precluding molecular weight determination. These observations are consistent with slow rates of initiation relative to propagation, with formation of very high molecular weight polymers. Such behavior is expected for **4a/4b**, the low solubility of which results in a low concentration of catalytically active species. Observation of similar results for **4c/8**, however, suggests an intrinsic initiation barrier, presumably associated with the stability of the $\text{Ru}_2(\mu\text{-Cl})_3$ moiety. The very low activity of the dinuclear alkylidene species, coupled with their ease

(27) The high activity that ensues for **4c/8** in CDCl_3 implies that the chlorocarbon-induced decomposition noted above does not occur at a rate competitive with metathesis. The higher stability of the dcybp complexes in C_6D_6 is offset by the slow rate of metathesis in this solvent, as previously noted.⁵

of formation, points toward a major catalyst deactivation pathway in this chemistry.

Conclusions

The foregoing describes an efficient route to the hydrido chloro dimer $\text{RuCl}(\text{dcypb})(\mu\text{-Cl})_2(\mu\text{-H})\text{Ru}(\text{dcypb})(\text{H}_2)$ and utilization of this species and the closely related chlororuthenium dimer $\text{RuCl}(\text{dcypb})(\mu\text{-Cl})_3\text{Ru}(\text{dcypb})(\text{N}_2)$ as atom-efficient entry points into dcypb chemistry. Dinuclear monoalkylidene, monovinylidene, and mono(hydroxy)vinylidene derivatives were isolated on reaction of the parent dimers with an excess of the appropriate alkyne. In no case were mononuclear or disubstituted dinuclear derivatives obtained. While formation of vinylidene and hydroxyvinylidene species of the type $\text{RuCl}(\text{dcypb})(\mu\text{-Cl})_3\text{Ru}(\text{dcypb})(\text{L})$ may be an artifact of the poor solubility of both the starting dimer and these products, formation of the analogous alkylidene complex from the soluble hydrido chloro precursor indicates a strong driving force for homodimerization of initially formed $\text{RuCl}_2(\text{dcypb})(\text{CHCH}=\text{CMe}_2)$ (**2d**). The low reactivity of the face-bridged alkylidene products, in conjunction with the facility with which such dimers are formed, affords insight into an important deactivation pathway accessible to catalysts of type **2**. We now have evidence that this process is likewise operative for the Grubbs catalyst $\text{RuCl}_2(\text{PPh}_3)_2(\text{CHCH}=\text{CMe}_2)$.^{23b} A related process, possibly involving loss of one bulky L donor per Ru, may apply to systems of type **1**. The accessibility of such deactivation pathways limits the advantages of enhanced catalyst lifetime anticipated from use of a robust late-transition-metal catalyst. Our current efforts focus on development of pseudohalide analogues of **2**, which have potential for enhanced selectivity as well as improved lifetime. The relative stability of model edge- and face-bridged complexes is also under investigation.

Experimental Section

General Procedures. All reactions were carried out at room temperature (22 °C) under N_2 using standard Schlenk or drybox techniques, unless stated otherwise. All reactions with H_2 were carried out under 1 atm pressure. Dry, oxygen-free solvents were obtained using an Anhydrous Engineering solvent purification system and stored over Linde 4 Å molecular sieves. CDCl_3 , C_6D_6 , and toluene- d_8 were dried over activated sieves (Linde 4 Å) and degassed by consecutive freeze/pump/thaw cycles. $\text{RuCl}(\text{dcypb})(\mu\text{-Cl})_3\text{Ru}(\text{dcypb})(\text{N}_2)$ (**3**)^{5b} and phenyldiazomethane²⁸ were prepared as previously described. Norbornene was purchased from Aldrich and distilled from sodium under N_2 . Potassium tri(*sec*-butyl)borohydride, 3,3-dimethyl-1-butyne, 3-chloro-3-methyl-1-butyne, 1,1-diphenyl-2-propyn-1-ol, and trimethylsilyl trifluoromethanesulfonate (TMS-OTf) were purchased from Aldrich and used as received. ^1H NMR (200, 300, or 500 MHz), ^{31}P NMR (121 MHz) and ^{13}C NMR (75 MHz) spectra were recorded on a Varian Gemini 200, Bruker Avance-300, or Bruker AMX-500 spectrometer. All 2D experiments were carried out on the Avance-300 instrument. IR spectra were measured on a Bomem MB100 IR spectrometer. Microanalyses were carried out inhouse, using a Perkin-Elmer Series II CHNS/O instrument, and by Guelph Chemical Laboratories Ltd., Guelph, Ontario, Canada.

(28) Creary, X. *Organic Syntheses*; Wiley: Toronto, 1990; Vol. VII, p 438.

$\text{RuCl}(\text{dcypb})(\mu\text{-Cl})_3\text{Ru}(\text{dcypb})(\text{C}=\text{CHBu}^t)$ (4a**).** An orange suspension of **3** (180 mg, 0.14 mmol) in 5 mL of benzene was treated with 3,3-dimethyl-1-butyne (52.2 μL , 0.32 mmol). The suspension was stirred at 22 °C for 12 h, over which time it darkened slightly but did not dissolve. Concentration and addition of pentane (2 mL) afforded more of the orange solid, which was filtered off, washed with pentane (3 \times 1 mL), and dried under vacuum. Yield: 161 mg (86%). ^1H NMR (CDCl_3): δ 3.06 (t, $\text{Ru}=\text{C}=\text{CHBu}^t$, $^4J_{\text{HP}} = 3.8$ Hz, 1H), 3.1–3.2 (br, aliphatic, 2H), 1.24 (s, $\text{C}(\text{CH}_3)_3$, 9H), 1.0–3.0 (br, aliphatic, 102H). $^{31}\text{P}\{^1\text{H}\}$ NMR (CDCl_3): δ 50.6, 49.6 (ABq, $^2J_{\text{PP}} = 37$ Hz), 45.9 (d, $^2J_{\text{PP}} = 23$ Hz), 40.1 (d, $^2J_{\text{PP}} = 23$ Hz). $^{13}\text{C}\{^1\text{H}\}$ NMR (C_6D_6): δ 352.1 (t, RuC , $^2J_{\text{CP}} = 16$ Hz), 119.7 (s, $\text{RuC}=\text{C}$), 33.8 (s, $\text{C}(\text{CH}_3)_3$), 15–45 (aliphatic). IR (Nujol): $\nu(\text{C}=\text{C})$ 1633 cm^{-1} . Anal. Calcd for $\text{C}_{62}\text{H}_{114}\text{Cl}_4\text{P}_4\text{Ru}_2$: C, 56.10; H, 8.66. Found: C, 56.35; H, 9.04.

$\text{RuCl}(\text{dcypb})(\mu\text{-Cl})_3\text{Ru}(\text{dcypb})(\text{C}=\text{CHC}(\text{OH})\text{Ph}_2)$ (4b**).** An orange suspension of **3** (98 mg, 0.075 mmol) and 1,1-diphenyl-2-propyn-1-ol (34 mg, 0.16 mmol) in 8 mL of benzene was stirred for 12 h at 22 °C, over which time it darkened to brown. Hexanes (4 mL) was added, and the brown solid was filtered off, washed with hexanes (3 \times 1 mL), and dried under vacuum. Yield: 97 mg (88%). ^1H NMR (C_6D_6): δ 7.51 (d, $^3J_{\text{HH}} = 6.5$ Hz, 4H, *o*- C_6H_5), 7.28 (t, $^3J_{\text{HH}} = 7.5$ Hz, 4H, *m*- C_6H_5), 7.18 (t, $^3J_{\text{HH}} = 7.1$ Hz, 2H, *p*- C_6H_5), 4.38 (br, $\text{Ru}=\text{C}=\text{CH}$, 1H), 3.99 (br, 1H, xch D_2O , OH), 0.8–3.5 (br, aliphatic, 104H). $^{31}\text{P}\{^1\text{H}\}$ NMR (C_6D_6): δ 51.5 (d, $^2J_{\text{PP}} = 38$ Hz), 50.1 (d, $^2J_{\text{PP}} = 38$ Hz), 44.7 (d, unresolved), 40.9 (d, unresolved). $^{13}\text{C}\{^1\text{H}\}$ NMR (C_6D_6): δ 308.7 (t, RuC , unresolved), 243.4 (s, $\text{RuC}=\text{C}$), 150.4 (s, $\text{RuC}=\text{C}=\text{C}$), 149.4–120.2 (aromatic), 53.1–14.0 (aliphatic). IR (Nujol): $\nu(\text{O}-\text{H})$ 3483; $\nu(\text{C}=\text{C})$ 1644 cm^{-1} . Anal. Calcd for $\text{C}_{71}\text{H}_{114}\text{Cl}_4\text{P}_4\text{Ru}_2$: C, 58.67; H, 8.04. Found: C, 59.07; H, 8.34.

$\text{Ru}(\text{H})(\text{dcypb})(\mu\text{-Cl})_2(\mu\text{-H})\text{Ru}(\text{dcypb})(\text{H}_2)$ (5**).** An orange suspension of **3** (20 mg, 31.4 μmol Ru) in C_6D_6 (1 mL) was stirred under 1 atm of H_2 for 5 min at 22 °C, following which a C_6D_6 solution (1 mL; H_2 -saturated) of KHB^tBu_3 (32 μL of a 1.0 M solution in Et_2O) was added by cannula. A clear, slightly darker orange solution formed within minutes. NMR analysis was carried out by transferring the solution by cannula into a Teflon-lined screw-cap NMR tube filled with H_2 . Attempts to isolate the products, or indeed to handle them in the absence of H_2 , resulted in extensive decomposition (NMR). We have reported the crystal structure of one of the decomposition products, $[\text{Ru}(\text{H})(\text{dcypb})(\mu\text{-Cl})_3\text{Ru}(\text{dcypb})(\text{N}_2)]$ (**7**).¹⁹ A few small crystals of **5** formed at the solvent–gas interface over several days under H_2 , one of which was found suitable for X-ray analysis. ^1H NMR (C_6D_6): δ 0.6–3.0 (m, aliphatic), –13.8 (s, *H*, H_2). ^{31}P NMR (C_6D_6): δ 65.1 (br s), 52.2 (br s). Hydride T_1 min (C_7D_8 , H_2 , 500 MHz, 284 K): 38 ms. IR (Nujol): $\nu(\text{Ru}-\text{H})$ 2102 (m), 2066 (m) cm^{-1} .

$\text{Ru}_2\text{Cl}_4(\text{dcypb})_2[\text{CHCH}=\text{C}(\text{CH}_3)_2]$ (4c** + **8**).** A suspension of **3** (186 mg, 0.29 mmol Ru) in 10 mL of toluene under H_2 was treated with KHB^tBu_3 (292 μL of a 1.0 M solution in Et_2O). Over 3 h at 22 °C the suspension gave way to a dark orange solution consisting solely of **5** (NMR evidence). Addition of a solution of 3-chloro-3-methyl-1-butyne (66 μL , 0.58 mmol) in 2 mL of toluene caused immediate darkening of the solution to green-brown. After 1 h of reaction, $^{31}\text{P}\{^1\text{H}\}$ NMR showed complete conversion to two products, in a ratio of 4:1. The major product can be unambiguously identified as $\text{RuCl}(\text{dcypb})(\mu\text{-Cl})_3\text{Ru}(\text{dcypb})(\text{CHCH}=\text{CMe}_2)$ (**4c**). The second product (**8**) is proposed to be an isomer containing a bridging alkylidene (see text). Identical results were obtained on use of a larger excess of the alkyne (20 equiv) or on carrying out the reaction at –35 °C. The solution was filtered through Celite and concentrated. Addition of hexanes resulted in a brown precipitate, which was filtered off, washed with pentane (5 \times 1 mL), and then reprecipitated from benzene–hexanes. Yield: 158 mg (82%). Repeated efforts to separate **4c** and **8** by reprecipitation from other solvent mixtures (using various combinations of hexanes, pentane, or 2-propanol with benzene,

toluene, or THF), or extraction were unsuccessful. ^1H NMR (C_6D_6): δ 16.92 (q, RuCH, $^3J_{\text{HH}} = 11.5$ Hz, $^3J_{\text{HP}} = 11.5$ Hz, **4c**), 15.83 (q, RuCH, $^3J_{\text{HH}} = 12.0$ Hz, $^3J_{\text{HP}} = 12.0$ Hz, **8**), 9.1 (m, RuCHCH, **4c** and **8**), 0.5–3.5 (br, aliphatic, **4c** and **8**). $^{13}\text{C}\{^1\text{H}\}$ NMR (C_6D_6): δ 308.6 (m, unresolved, RuC, **8**), 292.7 (t, RuC, $^2J_{\text{PC}} = 15$ Hz, **4c**). $^{31}\text{P}\{^1\text{H}\}$ NMR (C_6D_6): **4c**, δ 54.0 (br s), 46.1 (br s), 45.1 (br s), 42.9 (br s); **8**, δ 43.4 (s). $^{31}\text{P}\{^1\text{H}\}$ NMR (CDCl_3): **4c**, δ 59.0 (d, $^2J_{\text{PP}} = 39$ Hz), 46.9 (d, $^2J_{\text{PP}} = 26$ Hz), 43.7 (d, $^2J_{\text{PP}} = 39$ Hz), 40.5 (d, $^2J_{\text{PP}} = 26$ Hz); **8**, δ 44.4 (s). A new, unidentified species (δ 46.4 (d, $^2J_{\text{PP}} = 35$ Hz), 42.6 (d, $^2J_{\text{PP}} = 35$ Hz)) is also present in CDCl_3 , probably owing to reaction with the solvent, as crystals of $\text{Ru}_2\text{Cl}_5(\text{dcypb})_2$ ^{5b} form on longer standing. IR (Nujol): $\nu(\text{C}=\text{C})$ 1578 cm^{-1} . Anal. Calcd for $\text{C}_{61}\text{H}_{112}\text{Cl}_4\text{P}_4\text{Ru}_2$ (**4c** + **8**): C, 55.78; H, 8.60. Found: C, 55.08; H, 8.33. Crystals of **4c** were obtained by layering a toluene solution with hexanes.

General Procedure for Polymerization of Norbornene.

A solution of norbornene (34 mg, 0.36 mmol) in 299 μL of CDCl_3 was added to an NMR tube containing a CDCl_3 solution of the catalyst (1.6 μmol of Ru=C; 201 μL of an 8.1 mM stock solution). The reaction was monitored by ^1H NMR. Trimethylsilyl triflate or PhCHN_2 , if required, were added to the monomer solution prior to addition to catalyst (TMS-OTf, 1.6 μmol , 10 μL of a 0.16 M TMS-OTf solution in CDCl_3 ; PhCHN_2 , 0.2 μL , 1.6 μmol).

Structural Determination of **4c and **5**.** Suitable crystals were selected, mounted on thin glass fibers using paraffin oil, and cooled to the data collection temperature. Data were collected on a Bruker AX SMART 1k CCD diffractometer using 0.3° ω -scans at 0, 90, and 180° in ϕ . Unit cell parameters were determined from 60 data frames collected at different sections of the Ewald sphere. Semiempirical absorption corrections based on equivalent reflections were applied.²⁹ No symmetry higher than triclinic was observed for **4c** or **5**, and solution in the centrosymmetric option yielded chemically reasonable and

computationally stable results of refinement. The structures were solved by direct methods, completed with difference Fourier syntheses, and refined with full-matrix least-squares procedures based on F^2 . Cocrystallized solvent molecules were located in the asymmetric units of **4c** (half a molecule of *n*-hexane) and **5** (two molecules of benzene). The cocrystallized hexane molecule in **4c** is located at an inversion center.

In **5**, hydrogen atomic positions H(1), H(2), and H(3) were located from the difference map using low-angle data ($<15^\circ$). On the basis of trans bond distances, H(1) and H(2) were assigned disordered H/H₂ identities with a hydrogen occupancy of 1.5 each. The bridging hydride ligand H(3) and the 50/50 disordered H/H₂ sites H(1) and H(2) were refined with a riding model. All other non-hydrogen atoms were refined with anisotropic displacement parameters. All hydrogen atoms on organic moieties were treated as idealized contributions. All scattering factors and anomalous dispersion factors are contained in the SHELXTL 5.10 program library.³⁰

Acknowledgment. The kind assistance of Prof. Tze-Lock Chan (Chinese University of Hong Kong) in providing spectra of an authentic sample of the triene is gratefully acknowledged. This work was supported by the Natural Sciences and Engineering Research Council of Canada, the Canada Foundation for Innovation, and the Ontario Innovation Trust.

Supporting Information Available: Tables of crystal data and data collection and refinement parameters, atomic coordinates, bond lengths and angles, anisotropic displacement parameters, and hydrogen coordinates for **4c** and **5**. This material is available free of charge via the Internet at <http://pubs.acs.org>.

OM0110888

(29) Blessing, R. *Acta Crystallogr.* **1995**, *A51*, 33.

(30) Sheldrick, G. M. Bruker AXS, Madison, WI, 1997.